Tellus (1983), *35A*, 17–27

Linear non-divergent mass–wind laws on the sphere

By ROGER DALEY, *National Center for Atmospheric Research,*[1] *P.O. Box 3000, Boulder, Colorado 80307, U.S.A.*

(Manuscript received January 19; in final form April 15, 1982)

ABSTRACT

The properties of 3 types of linear non-divergent mass–wind laws on the sphere have been examined: linear-balance equation, spherical harmonic expansions of the linearized primitive equations, and Rossby–Hough expansions. Both the symmetric and antisymmetric non-zonal cases are examined. The results show that all 3 methods are virtually equivalent for the antisymmetric case, but differ considerably for the symmetric case. All 3 methods, whether derived from the primitive equations or from a filtering approximation, appear to be singular at the equator in the symmetric case.

1. Introduction

Linear mass–wind laws have played an important role in meteorology since the early 19th century. In particular, the geostrophic wind law, first formulated as the Buys-Ballot Law (1857), has been one of the cornerstones of modern theoretical meteorology. Linear mass–wind laws have also been very useful in meteorological observation, for obtaining the mass field from the wind or vice versa. At present these laws are widely used in an implicit sense in multivariate analysis procedures. Also, numerical prediction or climate simulation models satisfy (at least to lowest order) linear mass–wind relations of the types discussed here.

The simplest form of the geostrophic relationship is $\Phi = f\psi$. Here Φ is the geopotential, ψ is the streamfunction and f is the Coriolis parameter. If this equation were to be applied to the spherical case, where f varies with latitude, then it is clear that there will be difficulties at the equator where f becomes vanishingly small. In particular, calculating $\psi = f^{-1}\Phi$ may well be singular at the equator. It might be noted, however, that the nature of the singularity depends upon whether Φ is symmetric or antisymmetric with respect to the equator. Because f is antisymmetric, a symmetric Φ will generate an antisymmetric ψ and vice versa. If Φ is symmetric (i.e. non-zero at the equator except in special cases), then ψ will, in general, be singular at the equator. If Φ is antisymmetric (i.e. identically zero at the equator), then ψ need not be singular there.

The next most general form of the geostrophic relationship is the linear balance equation $\nabla^2\Phi = \nabla\cdot f\nabla\psi$. The linear balance equation (LBE) is the natural extension of the geostrophic relationship to the sphere, in that the latitudinal variation of the Coriolis parameter is properly accounted for. The spherical LBE has been extensively studied by Eliasen and Machenhauer (1965), Merilees (1968) and Baer (1977). Their analyses of the spherical LBE show that any *arbitrary* symmetric geopotential field will generate an antisymmetric streamfunction field whose kinetic energy is infinite. This result is presumably caused by the vanishing of f at the equator. However, an antisymmetric geopotential will produce a symmetric streamfunction whose kinetic energy is finite. (These results are for the non-zonal case; in the zonal case the kinetic energies of both symmetric and antisymmetric streamfunctions are finite.)

Another linear mass–wind relationship appro-

[1] The National Center for Atmospheric Research is sponsored by the National Science Foundation.

0280-6495/83/010017-11$2.50/0

priate for the sphere can be obtained from the Laplace tidal theory (Flattery, 1967; Longuet-Higgins, 1968; Kasahara, 1976). The Laplace tidal equations are obtained from the spherical primitive equations, linearized about a state of rest. In particular, the low frequency westward propagating solutions of the second kind (which we will refer to as Rossby–Hough modes) provide a useful mass–wind relationship. These modes appear to be in approximate geostrophic balance at higher latitudes. Because the Rossby–Hough solutions are obtained from the linearized spherical primitive equations (and not from a filtering approximation, like the LBE) they should provide a more general mass–wind relation. Wiin-Nielsen (1979)—hereafter referred to as WN—has investigated the mass–wind relation satisfied by these modes and shown that it is in many respects similar to that of the LBE, although there are substantial differences in the planetary scales.

There are also linear mass–wind relationships between the velocity potential χ and the geopotential Φ in the quasi-geostrophic theory and the tidal equations. These linear relationships (as discussed by Wiin-Nielsen, 1979) have some utility in the planetary scales, but in the synoptic scales the χ–Φ relationships are basically non-linear. Thus, we have decided to continue our attention to the ψ–Φ relationships.

It has long been known that the solution of the non-linear counterpart of the LBE (the so-called non-linear balance equation where Φ is specified and ψ is to be determined) can be difficult in the tropics. This problem, known as the ellipticity problem, occurs in regions of large positive geopotential anomaly and small Coriolis parameter. Only recently, however, it has been shown by Daley (1978) and Tribbia (1981) that the spherical primitive equation counterpart of the non-linear balance equation (as obtained from the non-linear normal mode theory) also has a type of ellipticity problem very similar to that in the non-linear balance equation. Thus, although the ellipticity problem may appear to have been circumvented by making use of the primitive equations, this is not really so.

The purpose of the present article is to show that there is a similar parallel between the LBE and the Rossby–Hough solutions of the tidal equations. Thus, in the present work, we will show that the linear mass–wind relationship satisfied by these truly global solutions of the linearized primitive equations appears to have a singularity at the equator. We will discuss both the symmetric and antisymmetric cases, but will confine the analysis to the non-zonal case. We will discuss both true Rossby–Hough functions and the normal modes of linearized spherical primitive equation spectral models (which are approximations to the Rossby–Hough modes).

2. Theory

The formulation of the problem will closely follow that of WN and consequently most of the details will be omitted here. As in WN, we consider the shallow water equations on a spherical earth. In general we shall use the notation defined in Daley (1981).

$$\frac{\partial}{\partial t}\nabla^2\psi + \frac{2\Omega}{a^2}\frac{\partial\psi}{\partial\lambda} + L(\chi) = 0, \tag{2.1}$$

$$\frac{\partial}{\partial t}\nabla^2\chi + \frac{2\Omega}{a^2}\frac{\partial\chi}{\partial\lambda} - L(\psi) + \nabla^2\Phi = 0, \tag{2.2}$$

$$\frac{\partial\Phi}{\partial t} + g\bar{H}\nabla^2\chi = 0, \tag{2.3}$$

$$L(\eta) = 2\Omega\left[\mu\nabla^2\eta + \frac{(1-\mu^2)}{a^2}\frac{\partial\eta}{\partial\mu}\right], \tag{2.4}$$

where ψ, χ, and Φ are the streamfunction, velocity potential, and geopotential, respectively, Ω is the earth's rotation rate, g is the gravitational constant, $\bar{H}$ is the equivalent depth, $\mu = \sin\phi$ where ϕ is the latitude, λ is the longitude, and a is the earth's radius.

As in WN we expand (2.1–2.3) in spherical harmonic functions (the un-normalized form is used here). Thus,

$$\begin{bmatrix}\psi\\ \chi\\ \Phi\end{bmatrix} = \sum_{m=-M}^{M}\begin{bmatrix}\psi^m(\mu)\\ \chi^m(\mu)\\ \Phi^m(\mu)\end{bmatrix}\exp(im\lambda - 2\Omega i\sigma t), \tag{2.5}$$

where

$$\begin{bmatrix}\psi^m(\mu)\\ \chi^m(\mu)\\ \Phi^m(\mu)\end{bmatrix} = \sum_{n=|m|}^{|m|+2N-1}\begin{bmatrix}\psi_n^m\\ i\chi_n^m\\ 2\Omega\Phi_n^m\end{bmatrix}P_n^m(\mu), \tag{2.6}$$

where m is the zonal wavenumber, n is the meridional wavenumber, $i = \sqrt{-1}$, the P_n^m are the associated Legendre functions of the first kind, σ is the frequency, and N,M define the truncation of the spherical harmonic series.

Eqs. (2.1–2.3) are reduced to a standard algebraic eigenvalue problem for $N \to \infty$ (for each m) by the insertion of expansions (2.5–2.6) and the use of the Galerkin procedure. The eigensolutions of this problem are known as Hough functions (Longuet-Higgins, 1968) and the corresponding eigenvalues are frequencies. The solutions can be divided into two classes—slowly westward propagating Rossby modes, and rapidly eastward and westward propagating gravity modes. It is only the Rossby modes which concern us here and these modes will be denoted as follows:

Eigenfrequency Eigenvector

$$\sigma_R^{lm} \qquad \begin{bmatrix} R_\psi^l(\mu, m) \\ R_\chi^l(\mu, m) \\ R_\Phi^l(\mu, m) \end{bmatrix} \quad 1 \leqslant l \leqslant 2L, \tag{2.7}$$

where σ_R^{lm} is the eigenfrequency, R stands for Rossby mode, and l is the meridional index number (usually ordered by increasing numbers of zero crossings). In general, we must have $L \leqslant N$.

Streamfunction, velocity potential, and geopotential fields can be expanded in Rossby–Hough modes just as they can in spherical harmonics. Thus,

$$\begin{bmatrix} \psi^m(\mu) \\ \chi^m(\mu) \\ \Phi^m(\mu) \end{bmatrix} = \sum_{l=1}^{2L} A_l^m \begin{bmatrix} R_\psi^l(\mu, m) \\ R_\chi^l(\mu, m) \\ R_\Phi^l(\mu, m) \end{bmatrix} \tag{2.8}$$

where A_l^m are the Rossby–Hough expansion coefficients.

We note that in Hough mode expansion, the Hough functions for ψ, χ, and Φ are all different, whereas the expansion coefficients are the same. This is the reverse of an expansion in Legendre functions and consequently ψ^m, χ^m, and Φ^m cannot be completely arbitrary.

Eq. (2.8) can be separated into 2 expansions—a symmetric expansion in which ψ is antisymmetric and χ, Φ are symmetric and an antisymmetric expansion in which the reverse is true. If we insert spherical harmonic expansions for ψ^m, χ^m, Φ^m and R_ψ^l, R_χ^l, R_Φ^l into (2.8) we obtain equation (11) of WN.

$$\mathbf{R}_\psi \mathbf{A} = \boldsymbol{\psi}, \tag{2.9}$$

$$\mathbf{R}_\Phi \mathbf{A} = \boldsymbol{\Phi}, \tag{2.10}$$

where $\mathbf{A}$ is the column vector of length L of Rossby mode amplitudes, $\boldsymbol{\psi}$, $\boldsymbol{\Phi}$ are the column vectors of length N of spherical harmonic coefficients of the streamfunction and geopotential respectively and $\mathbf{R}_\psi$, $\mathbf{R}_\Phi$ are $N \times L$ rectangular matrices which relate $\boldsymbol{\psi}$ and $\boldsymbol{\Phi}$ to $\mathbf{A}$. We will get different matrices $\mathbf{R}_\psi$, $\mathbf{R}_\Phi$ for each value of m and there will be separate symmetric and antisymmetric matrices. We will not discuss relations involving the velocity potential.

WN considered the case where $N = L$, which would occur in numerical models based on a finite spherical harmonic expansion. In the case of Hough functions, it takes many spherical harmonics to define each Hough function properly, so L would have to be smaller than N. In the latter case the relation between $\boldsymbol{\psi}$ and $\boldsymbol{\Phi}$ (the mass–wind law) can be obtained as follows: multiply both sides of (2.10) by $\mathbf{R}_\Phi^T$ (the transpose of $\mathbf{R}_\Phi$). The matrix $\mathbf{R}_\Phi^T \mathbf{R}_\Phi$ is an $L \times L$ positive definite matrix which is invertible. Thus,

$$\boldsymbol{\psi} = \mathbf{X}\boldsymbol{\Phi}, \tag{2.11}$$

where $\mathbf{X} = \mathbf{R}_\psi(\mathbf{R}_\Phi^T \mathbf{R}\mathbf{R}_\Phi)^{-1}\mathbf{R}_\Phi^T$.

The non-divergent mass–wind relationship implied by the LBE can be obtained by ignoring the χ terms in (2.2) and expanding in spherical harmonics (see WN and Moura, 1976).

In the case $m = 0$ (zonal flow) the solutions of the Laplace tidal operator satisfy the LBE. This case has been extensively studied by Eliasen and Machenhauer (1965) and Merilees (1968) so we will confine our attention to the non-zonal case where the various linear wind laws differ substantially.

The matrix $\mathbf{X}$ defines the mass–wind relation in terms of a spherical harmonic expansion, which is the natural geometric metric for the sphere. This is because spherical harmonic functions are the eigensolutions of the spherical Laplacian operator and a properly truncated expansion in these functions is independent of the earth's axis

3. Results

We will first calculate the mass–wind matrices $\mathbf{X}$ for the LBE and Rossby–Hough expansions in the same manner as WN. The symmetric and antisymmetric cases will be considered separately. We will then perform some real data calculations.

3.1. *The symmetric case*

Following WN we first generate the matrices **X** for the symmetric case (Φ symmetric, ψ antisymmetric). Throughout all this subsection we will display the results for zonal wavenumber $m = 1$.

Table 1 shows the matrix **X** for the case $N = L = 7$ of the LBE and is strictly comparable to Table 2 of WN. Any discrepancies between WN and the present work are probably due to different precision used in defining the physical constants of the problem. All blank matrix elements indicate zeros in this case. Table 1 defines the 7×7 upper left hand corner submatrix of an infinite lower triangular matrix.

Merilees (1968) and Baer (1977) discussed the matrix elements in Table 1. They demonstrated that if the series defining the geopotential field were terminated at some point N, then the series defining the streamfunction had the following properties. Firstly, no matter how brutally the geopotential field was truncated, the resulting streamfunction series *did not* terminate. The terms of the streamfunction series correspond to the columns of Table 1, which shows the first 7 terms in the series. Secondly, the terms of the series although individually decreasing with increasing n, defined a divergent series in the kinetic energy. Thirdly, components of the streamfunction with n greater than the smallest-scale non-zero component of the geopotential were virtually independent of the geopotential field. The fact that the kinetic energy becomes infinite if all the terms in the streamfunction series are included, might be attributed to the vanishing of f at the equator, although this has never been formally proved.

In Table 2 we show the matrix **X** for the case of the Laplace tidal equations using the spherical harmonic expansion truncated at $N = L = 7$. As in WN $m = 1$, $\bar{H} = 8800$ m and we show the symmetric case. The results are strictly comparable with Table 1 of WN. All blank matrix entries have an absolute value less than 0.0001. As in WN matrix entries for all but the largest scales are similar to those in Table 1.

The matrix **X** in Table 2 is no longer lower triangular, but the elements above the main diagonal are, in general, quite small. We see the matrix elements in Table 2 become increasingly similar to those of Table 1 as n increases, but that the magnitudes are always larger. Table 2 suggests that the streamfunction series generated by a truncated geopotential series would be similar to that of the LBE in Table 1. Thus, we can speculate that the series for the kinetic energy defined by the Laplace tidal equations (symmetric case) is probably also divergent. Unfortunately, we cannot

Table 1. *The matrix* **X** *as defined in eq. (2.11) for the case $m = 1$, symmetric of the LBE truncated at $N = L = 7$*

1.1111						
−0.4267	1.4400					
0.2415	−0.8150	1.5918				
−0.1604	0.5414	−1.0573	1.6790			
0.1165	−0.3930	0.7676	−1.2189	1.7355		
−0.0895	0.3020	−0.5899	0.9367	−1.3337	1.7751	
0.0715	−0.2415	0.4716	−0.7489	1.0663	−1.4192	1.8044

Table 2. *The matrix* **X** *as defined in eq. (2.11) for the case $m = 1$, symmetric of the Laplace tidal equations truncated at $N = L = 7$*

1.3316	−0.0253	0.0015				
−0.5123	1.4520	0.0007				
0.2901	−0.8220	1.5924				
−0.1927	0.5460	−1.0577	1.6790			
0.1399	−0.3964	0.7679	−1.2190	1.7355		
−0.1075	0.3046	−0.5901	0.9367	−1.3337	1.7751	
0.0860	−0.2435	0.4718	−0.7489	1.0663	−1.4192	1.8044

prove this as the terms of the series are not given in closed form.

In a numerical model, both the streamfunction and geopotential would probably be truncated at the same value of n. The $N \times N$ matrix shown in either Table 1 or 2 would correspond to this case.

Tables 1 and 2 were calculated as simple 7×7 matrices as in WN. In the case of the linear balance equation the matrix entries are independent of N. Table 2 for the truncated spherical harmonic approximation to the tidal equations is weakly dependent of the value of N. Thus if $N = L = 20$, the entries in Table 2 only change in the 6th decimal point and Table 2 is thus virtually independent of the spherical harmonic truncation (N).

So far, we have considered solutions to the Laplace tidal equations where $L = N$. This procedure is consistent with a numerical model based on a spherical harmonic expansion, but it has one drawback. The lowest order Rossby solutions in the case $L = N$ are fairly accurate, but the higher order Rossby modes (as $l \to L$) are increasingly inaccurate. (In gridpint models there may be spurious computational modes as well.) In the present case with a relatively large equivalent depth we are able to calculate the Rossby–Hough modes to sufficient accuracy if $N \geqslant 3L$. A numerical model using a Hough mode expansion has been constructed by Kasahara (1977) and a Hough function objective analysis scheme has been developed by Flattery (1967).

We show in Table 3, the case $L = 7$, $N = 3L$ ($m = 1$, symmetric) which defines the mass–wind relationship between the largest meridional scales for a Rossby–Hough expansion with the same number of degrees of freedom as in Table 2. This matrix is, of course, the upper left hand subset of a much larger matrix. We show the first 9 rows and columns of this matrix (the 7×7 subset is shown inside the dashed lines). It can be seen that the values of the matrix elements decrease rapidly for row or column numbers greater than L. Table 3 is quite different from Table 2. Not only are there large matrix elements above the main diagonal, but elements below the main diagonal decrease more rapidly with increasing n than in Table 2. This suggests that the wind field does not respond as much to the smaller scale geopotential field in this case. One might speculate that for a truncated Rossby–Hough expansion, the apparent difficulties at the equator would be less obvious than for a spherical harmonic expansion with the same number of degrees of freedom.

We can also consider the case for the Rossby–Hough expansion where L gets large. We show in Table 4 the case $L = 40$, $N = 3L$. We show only the 7×7 upper left hand corner of the matrix. It can be seen that Table 4 is very like Table 2 and very different from Table 3. The results suggest that a Rossby–Hough expansion and a spherical harmonic expansion of the Laplace tidal equations have the same asymptotic mass–wind relation. However, a Rossby–Hough expansion only produces the asymptotic tidal mass–wind law in the largest scales with the inclusion of a great many degrees of freedom. This is primarily a manifestation of the fact that we are choosing to examine the problem within the context of a spherical harmonic metric.

The results of this section show that in the symmetric case, the mass–wind law implied by the LBE and an equivalently truncated spherical harmonic expansion of the Laplace tidal equations

Table 3. *The matrix* **X** *as defined in eq. (2.11) for the case $m = 1$, symmetric of the Laplace tidal equations truncated at $L = 7$, $N = 3L$; the first 9 rows and columns are shown*

1.3308	−0.0229	−0.0031	0.0071	−0.0102	0.0136	−0.0173	0.0222	−0.0008
−0.5096	1.4444	0.0142	−0.0236	0.0336	−0.0447	0.0568	−0.0730	0.0027
0.2835	−0.8032	1.5554	−0.0579	−0.0824	0.1097	−0.1393	0.1792	−0.0067
−0.1798	0.5093	−0.9866	1.5661	0.1609	−0.2141	0.2719	−0.3498	0.0130
0.1180	−0.3341	0.6471	−1.0273	1.4626	0.3633	−0.4614	0.5936	−0.0221
−0.0735	0.2081	−0.4032	0.6401	−0.9113	1.2130	0.7140	−0.9186	0.0342
0.0366	−0.1037	0.2009	−0.3190	0.4542	−0.6045	0.7697	1.3313	−0.0509
−0.0013	0.0037	−0.0072	0.0115	−0.0163	0.0217	−0.0293	−0.0491	0.0019
		0.0001	−0.0002	0.0003	−0.0004	0.0005	−0.0009	

are quite similar, whereas an equivalently truncated Rossby–Hough expansion would produce a somewhat different mass–wind law.

3.2. *Antisymmetric case*

The simple example discussed in Section 1 suggests that there might be considerable differences between the symmetric and antisymmetric case. The results of this section will suggest that this is indeed so.

As in Section 3.1, we will consider the zonal wavenumber $m = 1$ situation with $\bar{H} = 8800$ m. As noted previously, in the antisymmetric case Φ is antisymmetric and ψ is symmetric.

In Table 5 we show the matrix $\mathbf{X}$ for the case $N = L = 7$ of the LBE. The conventions are the same as in Table 1. Table 5 defines an upper triangular matrix. This means that for a given geopotential truncation, the streamfunction series will always terminate and thus the kinetic energy will remain finite. We note, however, that the magnitude of the elements of the matrix increase for increasing n, which means that small-scale geopotential components will be given large weight in generating the streamfunction.

Table 6 shows the matrix $\mathbf{X}$ ($N = L = 7$) for the case of a truncated spherical harmonic expansion of the Laplace tidal equations and is the antisymmetric equivalent of Table 2. The convention regarding blank matrix entries is the same for Table 2. There are non-zero matrix entries below the main diagonal, but they are small in magnitude.

Table 7 shows the case $L = 7$, $N = 3L$ ($m = 1$, antisymmetric) which defines the mass–wind relationship between the largest meridional scales for a Rossby–Hough expansion with the same number of degrees of freedom as Table 6. This table is the antisymmetric counterpart of Table 3; thus the first 9 rows and columns of the matrix are shown. As in Table 3, the magnitude of the matrix

Table 4. *The matrix* $\mathbf{X}$ *as defined in eq. (2.11) for equations truncated at* $L = 40$, $N = 3L$; *the first 7 rows and columns are shown*

1.3316	−0.0253	0.0015				
−0.5123	1.4520	−0.0006				
0.2901	−0.8220	1.5923				
−0.1927	0.5460	−1.0577	1.6790	0.0001	−0.0001	0.0002
0.1399	−0.3964	0.7678	−1.2188	1.7354	0.0002	−0.0003
−0.1075	0.3046	−0.5900	−0.9365	−1.3334	1.7748	0.0005
0.0859	−0.2434	0.4716	−0.7486	1.0659	−1.4187	1.8037

Table 5. *Same as Table 1 except for the antisymmetric case*

6.000	−14.222	24.576	−36.685	50.322	−65.332	81.598
	3.111	−5.376	8.025	−11.008	14.291	−17.850
		2.640	−3.941	5.406	−7.018	8.765
			2.449	−3.359	4.361	−5.447
				2.346	−3.045	3.803
					2.281	−2.849
						2.237

Table 6. *Same as Table 2 except for the antisymmetric case*

5.172	−12.059	20.820	−31.076	42.628	−55.342	69.121
0.026	3.046	−5.261	7.854	−10.773	13.986	−17.469
	0.002	2.637	−3.936	5.398	−7.009	8.754
			2.449	−3.354	4.361	−5.447
				2.346	−3.045	3.804
					2.281	−2.849
						2.237

elements decrease rapidly for $n > L$. Note, however, that Table 7 is much closer to Table 6, than Table 3 is to Table 2.

Table 8 shows the case $L = 40$, $N = 3L$ and is the antisymmetric counterpart of Table 4. It can be seen that Tables 6, 7, and 8 are all quite similar, which is *not* the case with their symmetric counterparts.

The results of this section show that in the antisymmetric case, the mass–wind law implied by the LBE, an equivalently truncated spherical harmonic expansion of the Laplace tidal equations and an equivalently truncated Rossby–Hough expansion are all quite similar.

3.3. *Calculations with FGGE data*

Some of the tentative conclusions drawn in Sections 3.1 and 3.2 were examined using real wind and height data from the first special observing period of FGGE. The data were obtained from the FGGE IIIb analyses of 500 mb height and streamfunction for 0000 GMT, January 13, 1979.

These FGGE IIIb analyses were derived using the three-dimensional multivariate statistical interpolation scheme of Lorenc (1980). The analysis consisted of 2 parts. A first guess field was obtained from a previous integration of the non-linear ECMWF model (Burridge and Haseler, 1977) and analyzed increments were added to the first guess field to obtain the first analysis. The first guess field was *not*, in general, in any type of linear geostrophic balance, but the analyzed increments *were* (because a local linear geostrophic relationship was used in the statistical covariance models except at low latitudes). Thus, although a local linear geostrophic relationship had been used in the analysis procedure, the final FGGE IIIb analyses were unlikely to be in linear geostrophic balance.

The data was analyzed into spherical components truncated at rhomboidal 15 (R15). The resulting geopotential and streamfunction analyses are shown in Fig. 1. Fig. 1a is a latitude–longitude plot of the geopotential (m) with a contour interval of 40 m. Fig. 1b is a latitude–longitude plot of the streamfunction (10^5 m^2 s^{-1}) with a contour interval of 40×10^5 m^2 s^{-1}. We note that the zonal flow is not included in these plots. The correspondence between the 2 fields in the extratropics is obvious.

A streamfunction was calculated from the observed geopotential field using the $\mathbf{X}$ matrices defined in Section 2. The calculated streamfunction was then compared with the observed streamfunction. As noted above, both the observed streamfunction and geopotential were truncated at

Table 7. *Same as Table 3 except for antisymmetric case*

5.171	−12.054	20.820	−31.076	42.629	−55.270	72.462	−2.872	0.054
0.026	3.046	−5.262	7.854	−10.773	13.968	−18.313	0.726	0.014
	0.002	2.637	−3.936	5.399	−7.000	9.177	−0.364	0.007
			2.449	−3.359	4.355	−5.710	0.226	−0.004
				2.348	−3.041	3.987	−0.158	0.003
					2.279	−2.987	0.118	−0.002
					0.002	2.345	−0.095	0.002
						−0.091	0.004	
						0.002		

Table 8. *Same as Table 4 except for the antisymmetric case*

5.171	−12.059	20.820	−31.076	42.628	−55.342	69.121
0.026	3.046	−5.262	7.854	−10.773	13.986	−17.469
	0.002	2.637	−3.936	5.398	−7.009	8.574
			2.449	−3.359	4.361	−5.447
				2.346	−3.045	3.804
					2.281	−2.849
						2.237

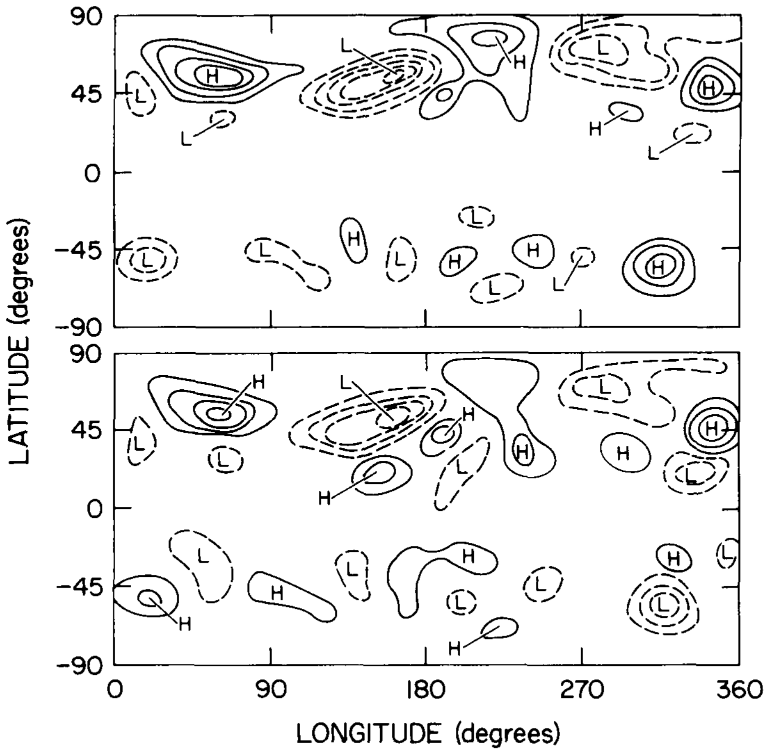

Fig. 1. Latitude–longitude plots of the R15 truncated height (a) and streamfunction (b) obtained from the FGGE IIIb analysis. The units are (m) and the contour interval is 40 m for the height field. For the streamfunction the units are 10^5 m^2 s^{-1} and the contour interval is 40×10^5 m^2 s^{-1}.

R15; the calculated streamfunction was not truncated. All zonal wavenumbers up to and including 15 were included, except for the zonal flow ($m = 0$). From the observed and calculated streamfunctions, the non-divergent winds were calculated and the r.m.s. vector wind error as a function of latitude was obtained. We note that there are 8 symmetric and antisymmetric modes for each zonal wavenumber in the *observed* geopotential and streamfunction.

Fig. 2 shows r.m.s. vector wind errors as a function of latitude for the symmetric and antisymmetric cases. We have shown for reference the total r.m.s. non-divergent vector wind (m s^{-1}) calculated from the *observed* streamfunction for the 2 cases (solid lines). All remaining lines on the graph indicate errors (i.e., observed wind minus calculated wind).

The dash lines in Fig. 2 indicate the LBE errors for the case $L = N = 8$. These results were obtained using matrices such as those in Tables 1 and 5 for each of the zonal wavenumbers. In this case there are 8 geopotential components and 8 observed and calculated streamfunction components. As is readily apparent, the error is small in high latitudes, but grows significantly near the equator, particularly in the symmetric case. In fact, the results are worthless equatorward of 20°. The dot-dash curve indicates the LBE error for the case $L = N = 16$. In this case there are 16 calculated streamfunction components generated from the 8 geopotential components, and the calculated streamfunction is not truncated. In the antisymmetric situation, the $L = N = 8$ and $L = N = 16$ calculations give virtually identical results and so the dashed and dash-dot curves are considered to coincide. In the symmetric situation, however, the $L = N = 16$ case results in much larger error near the equator. This result is consistent with the analysis of Sections 3.1 and 3.2.

We also calculated the streamfunction from the geopotential field using an equivalently truncated

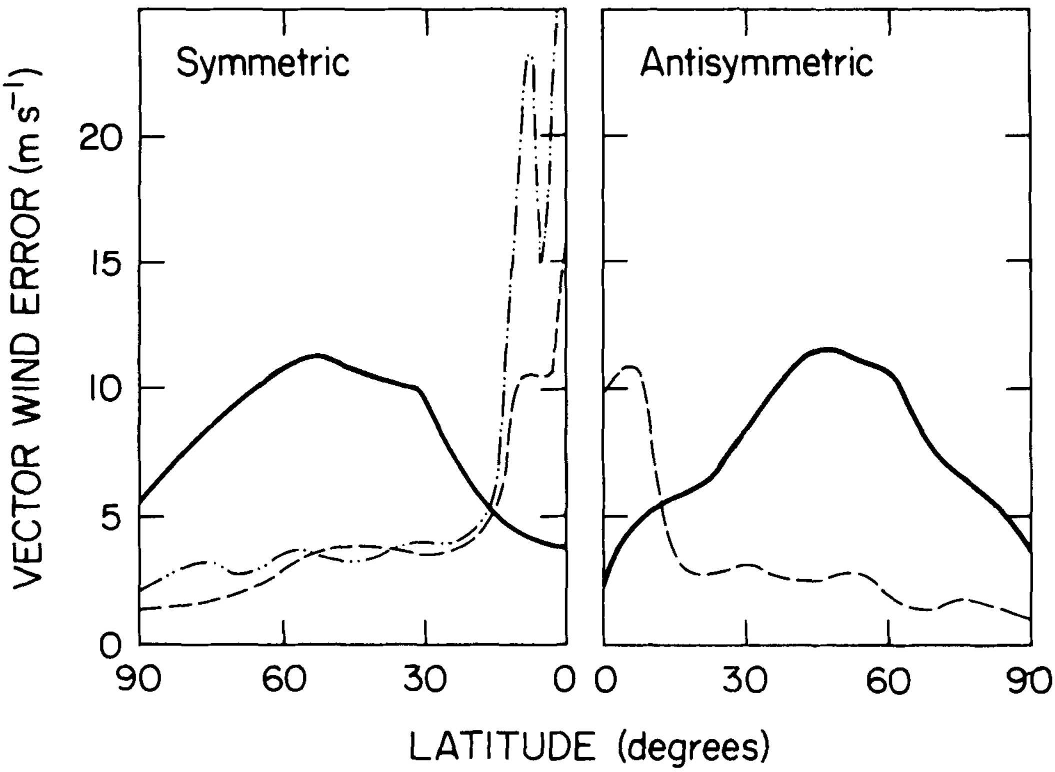

Fig. 2. R.m.s. vector non-divergent wind error for the symmetric and antisymmetric cases using the LBE. Solid line—r.m.s. non-divergent wind of the *observed* streamfunction. Dashed curve—vector wind error for $N = L = 8$ case. Dash-dot curve for the $N = L = 16$ case. The 2 cases are virtually identical in the antisymmetric case.

expansion of the Laplace tidal equations (i.e., with **X** matrices such as those in Tables 2 and 6). We considered both the cases $L = N = 8$ and $L = N = 16$ and the results were virtually identical to those obtained using the LBE (Fig. 2) and have consequently not been plotted.

Fig. 3, in the same format as Fig. 2, shows the same vector wind errors for the case of a truncated Rossby–Hough expansion. As in Fig. 2, the observed non-divergent vector wind (m s^{-1}) is plotted in the solid curve. We considered the 2 cases $L = 8$, $N = 3L$ (dashed line) and $L = 16$, $N = 3L$ (dot-dashed line). It is easy to see that the antisymmetric results are the same as in Fig. 2. For the symmetric situation the $L = 8$ case has less error at the equator than the corresponding $L = N = 8$ result of the LBE (Fig. 2). The same is true of the $L = 16$ calculation. However, we note that even for the symmetric Rossby–Hough modes, the error at the equator increases as L increases. This result might have been anticipated from Section 3.1.

The real data calculations of this subsection are consistent with the results of Sections 3.1 and 3.2. All methods (LBE, equivalently truncated spherical harmonic expansion of the Laplace tidal equations, and equivalently truncated Rossby–Hough expansions) give equally good results in the extratropics. All methods are equivalent for the antisymmetric case, and for a given antisymmetric geopotential field, produce virtually the same calculated streamfunction regardless of the number of degrees of freedom in the expansions. For the symmetric case, for a given geopotential field, all methods deteriorate near the equator as more degrees of freedom are allowed in the calculated streamfunction. For the symmetric case the LBE and spherical harmonic expansion of the Laplace tidal equations are much more similar to each other, than they are to the Rossby–Hough expansion.

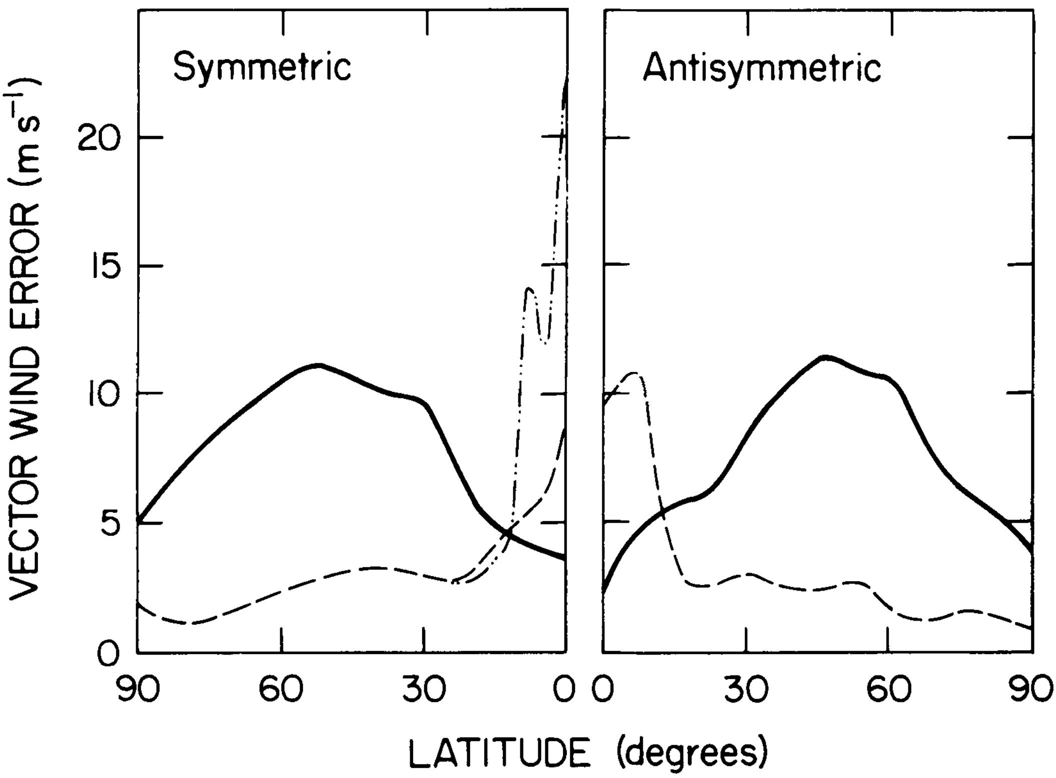

Fig. 3. Same as Fig. 2 except for Rossby–Hough expansion. Solid curve—as in Fig. 2. The dashed curve—$L = 8$, $N = 3L$. The dash-dot curve—$L = 16$, $N = 3L$.

4. Summary and conclusion

The properties of linear non-divergent mass–wind laws on the sphere have been examined. Of particular interest has been the behavior of these relationships in the vicinity of the equator. The 2 primary techniques used for the investigation of the problem are: (1) display of the spherical scale matrices relating the geopotential and streamfunction fields and (2) use of a FGGE IIIb data set to test the validity of the relationships.

Three linear mass–wind laws on the sphere were examined. The first was the linear balance equation (LBE) which is based on the quasi-geostrophic theory and is thus not expected to have any particular validity in the tropics. The other 2 mass–wind laws were based on the linearized primitive equations (i.e., the Laplace tidal equations) which are presumably valid everywhere. One of the tidal equation methods assumed a finite expansion in spherical harmonics, which is the procedure used in many of today's spectral numerical models. The other tidal equation method assumed a finite expansion in Rossby–Hough modes which are the low frequency eigensolutions of Laplace's tidal equations. The 2 tidal equation methods are not equivalent, except perhaps asymptotically, because each Rossby–Hough mode can only be represented as an infinite series of spherical harmonics.

Two cases were considered: the symmetric case in which the streamfunction is antisymmetric with respect to the equator and the geopotential is symmetric and the antisymmetric case where the reverse is true. Only the non-zonal case was considered as all 3 methods are equivalent for the zonal case. All results discussed below apply to equivalently truncated mass–wind relationships—that is, the number of degrees of freedom specified in the relationship is the same in each case.

We will discuss first the antisymmetric case, which is simpler. In the antisymmetric case all 3 methods—the LBE, a spherical harmonic expansion of the Laplace tidal equations and Rossby–Hough expansions give virtually the same result. Thus, from a prescribed antisymmetric geopotential field all 3 methods produce virtually the same symmetric streamfunction field regardless of the number of degrees of freedom allowed. The resulting streamfunction is reasonably accurate in the extratropics, but virtually worthless equatorward of 20°.

The symmetric case is more complicated. In this case, the LBE and a spherical harmonic expansion of the Laplace tidal equations (equivalently truncated) give virtually the same result. The results given by an equivalently truncated Rossby–Hough expansion differ somewhat from the other 2 methods in the symmetric case. Unlike the antisymmetric case, for a specified geopotential field *all* methods progressively deteriorate near the equator as more degrees of freedom are permitted in the mass–wind law. Thus, even a Rossby–Hough expansion produced a mass–wind relationship which appears to be singular near the equator in the symmetric case.

The results of the present study suggest that the linear mass–wind laws on the sphere, whether derived from quasi-geostrophic theory or from the primitive equations, are equally accurate in the extratropics, but are essentially invalid in the tropics. In the symmetric case, at least, all such mass–wind laws appear to be singular at the equator.

5. Acknowledgements

This work was partially supported by the National Oceanographic and Atmospheric Administration under P.O. No. NA81AAG00917. The author acknowledges useful conversations with J. Tribbia, F. Baer, and A. Kasahara. The manuscript was typed by J. Raese and M. Niemczewski, and the graphics were done by Stephanie Honaski and the NCAR Graphics Department.

REFERENCES

Baer, F. 1977. The spectral balance equation. *Tellus 29*, 107–115.

Burridge, D. and Haseler, J. 1977. A model for medium range weather forecasting—adiabatic formulation. ECMWF Technical Report No. 4, 45 pp.

Buys-Ballot, C. 1857. Note sur le rapport de l'intensité de la direction du vent avec les écarts simultanés du barometre. *Compt. Ren. 45*, 765–768.

Daley, R. 1978. Variational non-linear normal mode initialization, *Tellus 30*, 201–218.

Daley, R. 1981. Normal Mode initialization. *Rev. Geophys. Space Phys. 19*, 450–468.

Eliasen, E. and Machenhauer, B. 1965. A study of the fluctuations of the atmospheric flow patterns represented by spherical harmonics. *Tellus* 17, 220–238.

Flattery, T. 1967. Hough functions. Tech. Rept. No. 121, Dept. Geophys. Sci., The University of Chicago, 175 pp.

Kasahara, A. 1976. Normal modes of ultra-long waves in the atmpshere. *Mon. Wea. Rev. 104*, 669–690.

Kasahara, A. 1977. Numerical integration of the global barotropic primitive equations with Hough harmonic expansions. *J. Atmos. Sci. 34*, 687–701.

Longuet-Higgins, M. 1968. The eigenfunctions of Laplace's tidal equations over a sphere. *Philos. Trans. R. Soc. London, Ser. A. 262*, 511–607.

Lorenc, A. 1981. A global three-dimensional multivariate statistical interpolation scheme. *Mon. Wea. Rev. 109*, 701–721.

Merilees, P. 1968. On the linear balance equation in terms of spherical harmonics. *Tellus 20*, 200–202.

Moura, A. 1976. The eigensolutions of the linearized equations over a sphere. *J. Atmos. Sci. 33*, 877–907.

Tribbia, J. 1981. Normal mode balancing and the ellipticity condition. *Mon. Wea. Rev. 109*, 1751–1761.

Wiin-Nielsen, A. 1979. On normal mode initialization on the sphere. *J. Atmos. Sci. 36*, 2040–2048.